Chemistry–A European Journal
Research Article
doi.org/10.1002/chem.202401346
Chemistry Europe
European Chemical Societies Publishing
www.chemeurj.org

Double Chalcogen Bonding Recognition Arrays in Solution

Deborah Romito,[a] Hanspeter Kählig,[a] Paolo Tecilla,[b] Gabriele C. Sosso,[c] and Davide Bonifazi*[a]

N-substituted pyridino-based congeners of Ebselen, named here as Pyrselen, incorporating proximal Se and N atoms, undergo dimerization in solution and the solid state through a dual donor-acceptor arrangement of chalcogen bonding sites. Dimerization constants were measured within the 5–50 M^{-1} range. Computational studies on the dimers depict a notable charge-transfer contribution to the association, validating Pyrselen as an effective scaffold for designing chalcogen-bonding-based recognition motifs.

Introduction

In the last two decades, the non-covalent bonding interactions between Lewis-acidic chalcogen atoms and Lewis bases,[1] named Chalcogen Bonding Interactions (ChBIs),[2] have found growing interest in chemistry.[3] ChBIs have been widely used in the solid state,[4] for crystal engineering,[5] and to control the self-assembly of functional materials.[6] The exploitation of ChBIs in solution has steadily increased,[7] particularly in asymmetric syntheses,[8] annulation reactions,[9] catalysis,[10] and ion transport.[11] One of the seminal examples in molecular recognition includes the benzo-2,1,3-chalcogenadiazole scaffold[12] (Figure 1) used for anion binding (e.g., Cl^-, Br^-, I^- and NO_3^- with K_a values as high as $10^6\ M^{-1}$ for Cl^-).[11a] Benzo-2,1,3-telluradiazole moieties formed dimers in the gas phase as detected by mass spectrometry[13] and in solution as a telluradiazolynium congener using electrochemistry and EPR.[14] Supramolecular dimeric capsules comprising resorcin[4]arene cavitands with benzo-2,1,3-chalcogenadiazole moieties were also engineered.[15] In this architecture, sixteen concurrent Te···N ChBs established by the benzotelluradiazole units synergistically promoted the dimerization, displaying an exceptional K_d value of $\approx 10^7\ M^{-1}$. Chalcogenazoloxide-based recognition motifs were also developed, and cyclic oligomers formed both in the solid state and solution.[16] If one excludes Diederich's dimeric capsules, the development of programmed molecular modules undergoing ChBI-driven association in solution remains elusive. No conclusive data has been reported so far demonstrating the self-assembly of neutral recognition heterocycles in solution through ChBIs. This represents an obstacle to using ChBIs to engineer functional architectures outside crystal engineering.[3c,17]

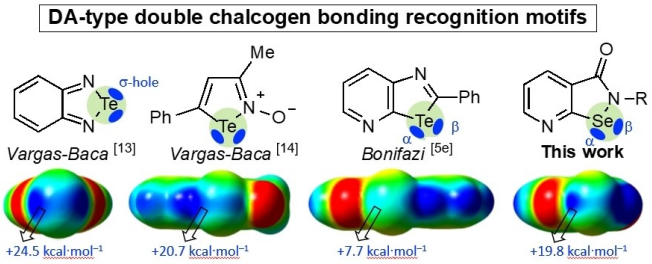

Figure 1. Side view of ESP maps (plotted with an isovalue of 0.01 a.u from Gaussian09 at B97-D3/def2-TZVP level of theory, $V_{s,max}$ in kcal mol^{-1})[11a] of *a)* classical synthons establishing DA-type ChBIs and of *b)* Pyrselen $\mathbf{1}_i$.

The effectiveness and persistency of ChB-based recognition motifs to undergo association relies on the specific proximity of the ChB donor and acceptor sites in the scaffold, as it allows multiple ChBs to take place (Figure 1). Building on this concept, in the last years, we have studied the chalcogenazolo pyridine (CGP) heterocycle, embodying N and chalcogen atoms proximal to each other as recognition unit persistently undergoing dimerization in the solid state through double Ch···N interactions involving either Se or Te atoms.[5e,18] Regrettably, such a dimerization does not manifest in $CDCl_3$ or CD_2Cl_2 solutions. Thus, the need arises to develop a novel scaffold capable of expressing stronger ChBIs. Considering the low Lewis acidity of the Te and Se atoms in the CGP moiety, one could devise a framework in which the chalcogen atom is considerably electron-depleted.

Drawing inspiration from the crystal structure of Ebselen,[19] in which molecules undergo intermolecular Se···O ChBs as short as covalent bonds, we conjectured that a selenazol-3-one moiety fused to a pyridyl ring in an Ebselen-like scaffold (Figure 1, named as Pyrselen) could feature a sufficiently depleted chalcogen atom to undergo dimerization through double ChBIs in solution. We calculated the Electrostatic Surface Potential (ESP) map to validate the design. We estimated the

[a] Dr. D. Romito, Prof. Dr. H. Kählig, Prof. Dr. D. Bonifazi
Department of Organic Chemistry, Faculty of Chemistry, University of Vienna, Währinger Straße 38, 1090 Vienna, Austria
E-mail: davide.bonifazi@univie.ac.at
[b] Prof. Dr. P. Tecilla
Dipertimento di Scienze Chimiche e Farmaceutiche, Università degli Studi di Trieste, Via Giorgieri 1, 34127 Trieste, Italy
[c] Prof. Dr. G. C. Sosso
Department of Chemistry, University of Warwick, CV4 7AL Coventry, UK

Supporting information for this article is available on the WWW under https://doi.org/10.1002/chem.202401346

value ($V_{s,max}$) at the point of the highest charge for both selenium donor and acceptor atoms. The chalcogen atom features two σ-holes(α) and σ-holes(β), with $V_{s,max}$ values of about +19 and +8 kcal mol^{-1}, respectively, which are significantly higher than those of the CGP moiety.[4a] The *N*-lactam-linkage considerably depletes the Se atom, enhancing the σ-holes. As far as the pyridyl *N*-atom is concerned, similar values $V_{s,max}$ (−28.7 and −27.2 kcal mol^{-1}) for both CGP and Pyrselen motifs were respectively found.

Results and Discussion

Synthesis of Pyrselen Derivatives

The synthesis of pyridyl derivatives $\mathbf{1}_i$ was inspired by the *Młochowski*'s protocol (Scheme 1).[20] ^{t}Butyl ester **3** was first prepared in 61% yield from 2-chloronicotinic acid **2** with refluxing $SOCl_2$ followed by the addition of ^{t}BuOK in dry THF. The addition of a THF solution of **3** to a solution of Li_2Se_2, prepared *in-situ* upon the addition of Se^0 to a dark green solution of activated Li^0 and 4,4′-di-*t*-butyl-diphenylene in THF,[21] afforded diselenide **4** in 33% yield after 72 hours. The deprotection of the ^{t}butyl moieties with CH_3SO_3H in CH_2Cl_2 gave dicarboxylic acid **5** in 96% yield. Finally, reaction of **5** with $SOCl_2$ followed by the addition of a CH_2Cl_2 solution containing NEt_3 and the given amine, RNH_2, afforded Pyrselen derivatives $\mathbf{1}_i$ from moderate to excellent yields. Notably, the lowest yields were achieved when F–containing amines were employed (23% for $\mathbf{1}_F$, 21% for $\mathbf{1}_{3F}$, respectively), whereas trimethoxyaniline gave product $\mathbf{1}_{3Met}$ in 88% yield. All compounds were characterized by ^{1}H, ^{19}F, ^{13}C and ^{77}Se NMR, IR and HR-MS spectrometry. The latter technique already anticipated the occurrence of dimerization in solution, since the characterization spectra depict the dimer formation for almost all the Pyrselen derivatives. Elemental analysis was not performed because the presence of Se interferes with the outcome due to the formation of oxides upon combustion. Purity was assessed by NMR to be at least 95%. In the case of compound $\mathbf{1}_{3F}$, due to the limited solubility, the recorded ^{1}H NMR spectra show a low signal-to-noise ratio and cannot be used to determine the purity of the compound.

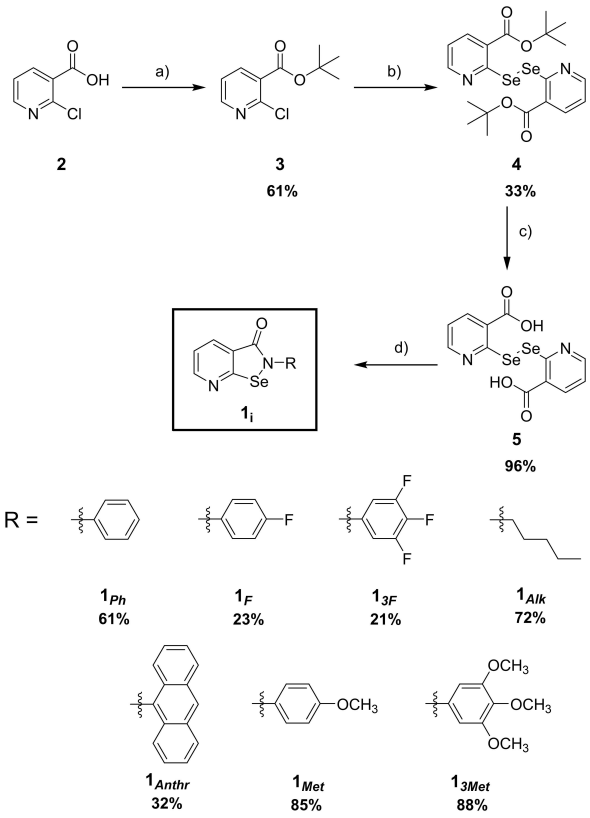

Scheme 1. Synthesis of Pyrselen derivatives 1_i. Reagents and conditions: *a)* $SOCl_2$, 78 °C; 4 h; 2. *t*-BuOK, THF, −15–25 °C, 16 h; *b)* Li_2Se_2, THF, −15–25 °C, 72 h; *c)* CH_3SO_3H, CH_2Cl_2, 25 °C, 16 h; *d)* 1. $SOCl_2$, DMF, 85 °C, 6 h; 2. $SOCl_2$, DMF, 85 °C, 16 h; 3. RNH_2, NEt_3, CH_2Cl_2, −15 (−40 °C for 1_F and 3_F) to 25 °C, 16 h.

X-Ray Diffraction Analysis

All pyridyl derivatives but $\mathbf{1}_F$, which is scarcely soluble in organic solvents, could be crystallized, yielding single crystals suitable for X-ray analysis. All molecules undergo dimerization, $(\mathbf{1}_i)_2$, by forming double Se···N ChBs (Figure 2).[22] Generally, the average Se···N contact length is of ~2.58 Å, almost 1 Å shorter than Σr_{vdW} (3.45 Å)[23] and is unaffected by the *N*-substituent. The 4-H atom of the phenyl rings in $(\mathbf{1}_{Ph})_2$ establishes weak intermolecular hydrogen bonds (HBs) with the carbonyl O atoms ($d_{C3\cdots O1}$ = 3.144 Å; $d_{C15\cdots O2}$ = 3.149 Å – Figure S35a), giving rise to a supramolecular polymer-like arrangement. Similarly, multiple HBs are present in the crystal structures of MeO-bearing derivatives $\mathbf{1}_{Met}$ and $\mathbf{1}_{3Met}$. In these cases, dimers $(\mathbf{1}_{Met})_2$ and $(\mathbf{1}_{3Met})_2$ are bridged through the carbonyl O atoms ($d_{O1\cdots C13}$ = 3.417 Å for $\mathbf{1}_{Met}$ – Figure S36a) and the methoxy O atoms (average $d_{O\cdots C}$ = 3.29 Å for $\mathbf{1}_{3Met}$ – Figure S36b), respectively. At last, for molecules $\mathbf{1}_{Alk}$ and $\mathbf{1}_{Anthr}$, vdW interactions seem to be the significant component ruling the organization of the dimers. While dimer $(\mathbf{1}_{Alk})_2$ forms hydrophobic domains through the alkyl interdigitation (Figure S37), the anthracenyl moieties in $(\mathbf{1}_{Anthr})_2$ establish multiple $\pi\cdots\pi$ stacking interactions ($d_{\pi\cdots\pi}$ = 3.3 Å), ultimately giving a supramolecular polymer-like organization (Figure S38).

Self-Assembly of Pyrselen in Solution

Next, we investigated self-assembly properties in a solution of $\mathbf{1}_i$ by measuring their homomolecular association strength, i.e., dimerization constant K_d, through ^{77}Se NMR dilution studies in $CDCl_3$ at 298 K. The scarce solubility of molecules $\mathbf{1}_{Anthr}$ and $\mathbf{1}_{3F}$ in $CDCl_3$ prevented us from studying them. NMR experiments (Figure 3) showed a fast association equilibrium depicting, upon dilution, a progressive downfield shift ($\Delta\delta_{Se}$) of the ^{77}Se resonance of ~25 ppm for all the derivatives (*i.e.*, the δ_{Se} of the Se-atoms shifts from 940 to 976 ppm for $(\mathbf{1}_{Ph})_2$, Figure 3). Smaller, yet aligned with the expectations, upfield shifts were

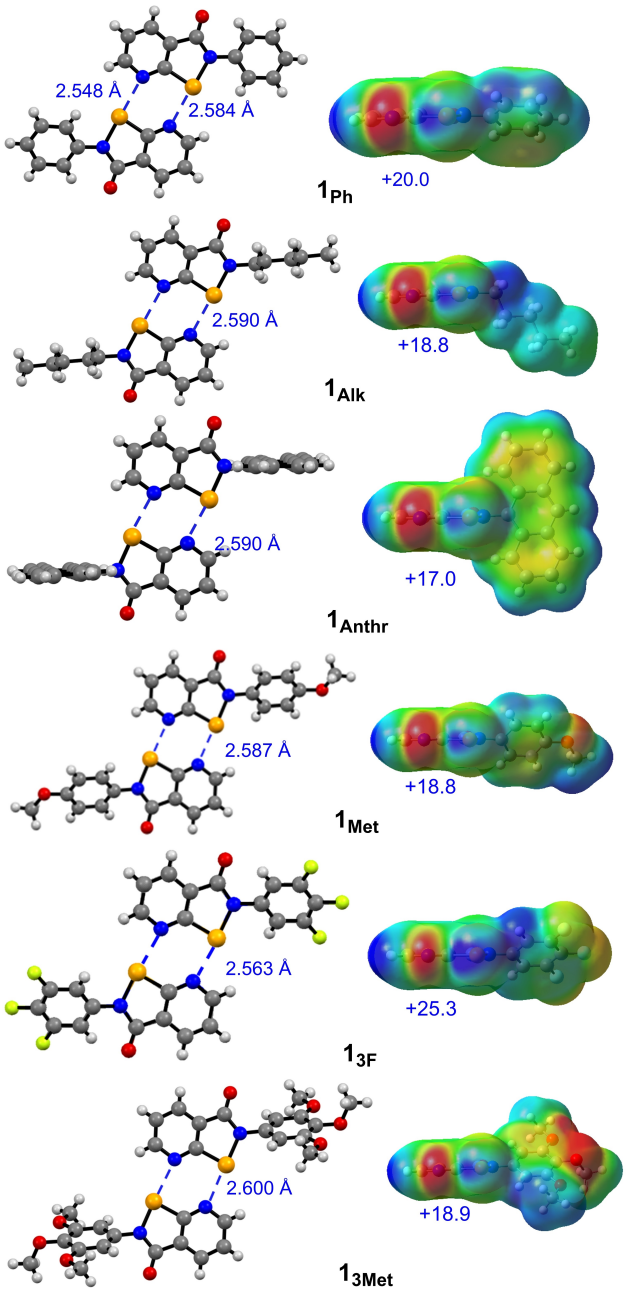

Figure 2. Left: crystal structures of selected Pyrselen dimers. Space groups: $Pca2_1$ ($\mathbf{1}_{Ph}$), C2/c ($\mathbf{1}_{Alk}$), P-1 ($\mathbf{1}_{Anthr}$), $P2_1/c$ ($\mathbf{1}_{Met}$), P-1 ($\mathbf{1}_{3F}$), $P2_1/n$ ($\mathbf{1}_{3Met}$). Right: ESP maps (plotted with an isovalue of 0.01 a.u.), depicting the values (kcal mol^{-1}) of $V_{s,max}$ for the σ-holes(α).[22]

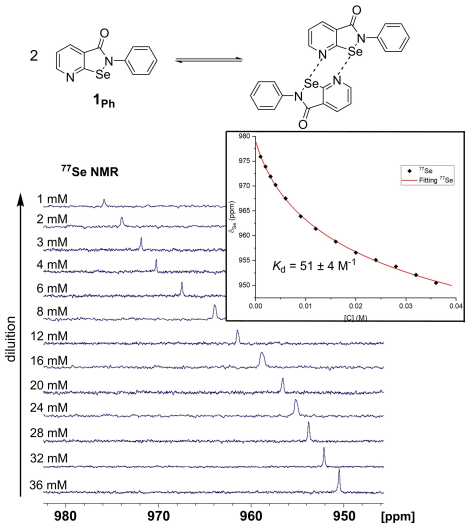

Figure 3. Overlapped ^{77}Se NMR (115 MHz) spectra for $CDCl_3$ solutions of $\mathbf{1}_{Ph}$ upon progressive dilution at 298 K; Inset: δ_{Se} *vs* concentration fitted to a 1:1 dimerization model.

observed for the pyridyl protons (averaged total $\Delta\delta_H =$ 0.039 ppm for $(\mathbf{1}_{Ph})_2$, see Figure S39). Fitting the ^{77}Se NMR dilution data to a 1:1 dimerization model,[24] the homomolecular association constants were found to be 51 ± 4, 30 ± 3, 28 ± 2, 15 ± 1, and 5.3 ± 0.8 M^{-1} for dimers $(\mathbf{1}_{Ph})_2$, $(\mathbf{1}_F)_2$, $(\mathbf{1}_{Met})_2$, $(\mathbf{1}_{3Met})_2$, and $(\mathbf{1}_{Alk})_2$, respectively. Reproducibility was assessed for dimers $(\mathbf{1}_{Ph})_2$ and $(\mathbf{1}_{Alk})_2$ with duplicate dilution experiments giving mean K_d values of 57.5 M^{-1} (s.d. 9.2) and 5.05 M^{-1} (s.d. 0.41), respectively. Generally, the dimerization values are small, with the *N*-aryl-bearing complexes featuring the stronger associations. The presence of electron-donating *N*-moiety weakens the dimerization constants, with the *N*-alkyl dimer $(\mathbf{1}_{Alk})_2$ showing the lowest stability (one order of magnitude weaker than that of $(\mathbf{1}_{Ph})_2$). Notably, the increasing donating effect at the *N*-substituent lowers the $V_{s,max}$ value of the σ-hole(α), ultimately weakening the ChBIs. Aiming at shedding further light onto the enthalpic and entropic contributions ruling the association of these dimers, van't Hoff analysis of variable temperature (VT) experiments were performed with 20 mM solutions of $\mathbf{1}_{Ph}$ and $\mathbf{1}_{Alk}$ in $CDCl_3$. Considering the negligible difference in the entropic loss for the dimerization of $\mathbf{1}_{Ph}$ and $\mathbf{1}_{Alk}$ (ΔS: −94 *vs* −81 J K^{-1} mol^{-1}, respectively), one can reasonably attribute the different stability of $(\mathbf{1}_{Ph})_2$ and $(\mathbf{1}_{Alk})_2$ to the enthalpic component (35 and 27 KJ mol^{-1} – Table S7). At last, the dimerization of $\mathbf{1}_{Ph}$ was screened in solvents with different polarities, namely CD_2Cl_2, and a 1:1 CD_2Cl_2/toluene mixture (due to the limited solubility of $\mathbf{1}_{Ph}$ in toluene). As one could anticipate,[3d] the polarity of non-coordinating solvents has a negligible influence on the association strength, with similar K_d values in CD_2Cl_2 and $CDCl_3$ (~50 M^{-1}) and a slightly lower association strength (~23 M^{-1}) in the mixed-solvents system (Figure S62). Although the measured dimerization constants are low, it is worth noting that they are comparable to the association constant of A/T complementary DNA base pairs (about 130 M^{-1} in $CHCl_3$, two hydrogen bonds) and, therefore, they may well be exploited in the design of cooperative supramolecular assemblies.[25]

Computational Studies

The nature of the ChB-based dimer developed by Pyrselen derivatives was further investigated by density functional theory (DFT) calculations (ESI for methodological details), starting with the determination of the interaction energies in the gas phase of phenyl-, alkyl- and anthracenyl-containing derivatives $\mathbf{1}_{Ph}$, $\mathbf{1}_{Alk}$, and $\mathbf{1}_{Anthr}$, using different exchange-correlation (XC) func-

tionals. The addition of dispersion corrections significantly increased the interaction energy (Figure S68). However, notwithstanding the choice of the specific XC functional, we found the strongest association for phenyl-containing compound $\mathbf{1}_{Ph}$. In contrast, alkyl-functionalized $\mathbf{1}_{Alk}$ is marked by the weakest interaction energy, as observed experimentally. We also calculated the different contributions (E_{frz}, E_{Pol}, and E_{Cov} for the frozen density, polarization, and covalent contribution, respectively) to the interaction energies of the dimers, by means of the ALMO-EDA framework[26] (ESI for details).

An illustrative example (Figure 4a) is reported for compound $\mathbf{1}_{Ph}$ (the other derivatives show an analogous trend). The E_{frz} component becomes repulsive as the two molecules get closer (starting from ~3 Å, due to the sizeable vdW radius of the Se atoms), while at the same time, the stabilization due to polarization (E_{Pol}) and charge transfer (E_{Cov}) increases. We estimated the contribution of charge transfer (CT) to be ~40 millielectrons (mē) at around the dimer equilibrium distance (Figure S68). To put this number into context, the extent of CT for the water dimer (computed via the same ALMO-EDA framework) is 0.1–5 mē.[27] In Figure 4b, we report the electron density ρ as a contour map projected onto the molecular plane for the $\mathbf{1}_{Ph}$ dimer at the equilibrium distance of 2.6 Å (estimated from the solid-state double ChBIs). Note the accumulation of ρ along the path connecting the Se and N atoms (Figure 4c, in yellow and green, respectively). Indeed, the bonding charge density difference $\Delta\rho$ is indicative of the emergence of significant charge transfer from the Se to the N atoms, with a net accumulation of electron density (red regions) along the direction of the N···Se bonding path.

Conclusions

To conclude, a Pyrselen-based recognition motif that undergoes association in solution has been engineered. Employing XRD analysis and ^{1}H and ^{77}Se NMR spectroscopies, it has been demonstrated that the module persistently undergoes dimerization through double ChB interactions both in the solid state and in solution. Association constants within the interval between 5 and 50 M^{-1} in $CDCl_3$ were measured, and van't Hoff analyses showed that the association is mainly governed by the enthalpic component. DFT calculations have identified a significant charge transfer component to the dimer ChBIs. Despite the relatively weak association constants, we anticipate this work will be an initial step towards establishing multiple-chalcogen-bonding recognition modules. Capitalizing on the multifaceted nature of ChBIs, we envision the development of recognition motifs displaying progressively stronger association constants, paving the way for their application in various self-assembly-oriented contexts.

Experimental Section

Methods and Instruments

Thin layer chromatography (TLC) was conducted on pre-coated aluminum sheets with 0.20 mm *Merck Millipore* Silica gel 60 with fluorescent indicator F254. *Column chromatography* used *Merck Gerduran* silica gel 60 (particle size 40–63 μm). ***Melting points*** (mp) were measured on a *Gallenkamp* apparatus in open capillary tubes. ***Nuclear magnetic resonance:*** (NMR) spectra were recorded on a Bruker Fourier 300 MHz spectrometer equipped with a dual (^{13}C, ^{1}H) probe, a Bruker AVANCE III HD 400 MHz NMR spectrometer equipped with a Broadband multinuclear (BBFO) SmartProbe™, a Bruker AVANCE III HD 500 MHz Spectrometer equipped with Broadband multinuclear (BBO) Prodigy CryoProbe or a Bruker AV III HDX 700 MHz NMR spectrometer (Bruker BioSpin, Rheinstetten, Germany) with a quadruple (^{1}H, ^{13}C, ^{15}N ^{19}F) inverse helium cooled cryo probe. ^{1}H spectra were obtained at 300, 400, 500, 600, or 700 MHz, ^{13}C{^{1}H} spectra were obtained at 75, 100, 125, 150, or 175 MHz NMR, and ^{19}F spectra were obtained at 376, 470, and 659 MHz. All spectra were obtained at rt. Chemical shifts were reported in ppm relative to tetramethylsilane using the residual solvent signal for ^{1}H or the solvent signal for ^{13}C as an internal reference ($CDCl_3$: $\delta_H = 7.26$ ppm, $\delta_C = 77.16$ ppm; C_6D_6: $\delta_H = 7.16$ ppm, $\delta_C = 128.06$ ppm). Chemical shifts for ^{19}F are reported on a unified scale relative to ^{1}H using the Ξ value for $CDCl_3$.[28] Coupling constants (*J*) were given in Hz. Resonance multiplicity was described as *s* (singlet), *d* (doublet), *t* (triplet), *dd* (doublet of doublets), *dm* (doublet of multiplets), *q* (quartet), *m* (multiplet) and *bs* (broad signal). Carbon spectra were acquired with ^{1}H decoupling. ^{77}Se NMR experiments were either recorded on a Bruker AV III HDX 700 NMR spectrometer (Bruker BioSpin, Rheinstetten, Germany) equipped with a broad band observe probe or on a Bruker AV III 600 NMR spectrometer using an N_2-cooled broad band observe cryoprobe. The resonance frequency for ^{77}Se was 133.58 MHz or 114.48 MHz, respectively. ***Infrared spectra*** (IR) were recorded on a

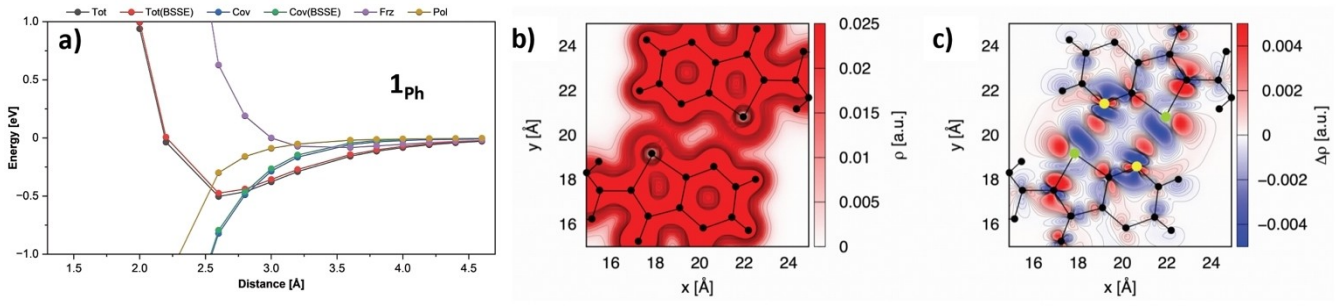

Figure 4. a) Contributions to the total interaction energy (Tot) for $(\mathbf{1}_{Ph})_2$ as a function of the intermolecular distance; Frz, Pol and Cov refer to the frozen density, polarization, and covalent contribution terms, respectively (ESI); the results accounting for the basis set superposition error (BSSE, see ESI) are also reported. b) Contour map of the electron density ρ projected onto the molecular plane xy. c) Electron density difference Δρ, calculated as the difference between the electron density of the dimer and that of the two monomers (Se and N atoms in green and yellow, respectively).

Shimadzu IR Affinity 1S FTIR spectrometer with a diamond monocrystal in ATR mode. ***Mass spectrometry:*** (i) High-resolution ESI mass spectra (HRMS) were performed on a Waters LCT HR TOF mass spectrometer in the positive or negative ion mode. ***X–ray measurements:*** The X-ray intensity data of $\mathbf{1_{Ph}}$, $\mathbf{1_{Alk}}$, $\mathbf{1_{Anthr}}$, $\mathbf{1_{Met}}$, and $\mathbf{1_{3Met}}$ were measured on Bruker D8 Venture diffractometer equipped with multilayer monochromator, Mo and Cu K/α INCOATEC micro focus sealed tubes and Oxford cooling system. The structures were solved by Direct Methods and Intrinsic Phasing. Non-hydrogen atoms were refined with anisotropic displacement parameters. Hydrogen atoms were inserted at calculated positions and refined with a riding model. The following software was used: Bruker SAINT software package[29] using a narrow-frame algorithm for frame integration, SADABS[30] for absorption correction, OLEX2[31] for structure solution, refinement, molecular diagrams, and graphical user interface, Shelxle[32] for refinement and graphical user interface SHELXS-2015[32] for structure solution, SHELXL-2015[33] for refinement, Platon[34] for symmetry check. Data collections $\mathbf{1_{3F}}$ were performed at the X-ray diffraction beamline (XRD1) of the Elettra Synchrotron (Trieste, Italy).[35] The crystals were dipped in NHV oil (Jena Bioscience, Jena, Germany) and mounted on the goniometer head with nylon loops (MiTeGen, Ithaca, USA). Complete datasets were collected at 100 K (nitrogen stream supplied through an Oxford Cryostream 700). Data were acquired using a monochromatic wavelength of 0.70 Å through the rotating crystal method on a Pilatus 2 M hybrid-pixel area detector (DECTRIS Ltd., Baden-Daettwil, Switzerland). The diffraction data were indexed and integrated using XDS.[36] The structure was solved with Olex2[37] by using ShelXT[38] structure solution program by Intrinsic Phasing and refined with the ShelXL[39] refinement package using least-squares minimization. In the last cycles of refinement, non-hydrogen atoms were refined anisotropically. Hydrogen atoms were included in calculated positions, and a riding model was used for refinement. Crystal data, data collection parameters, and structure refinement details are given in Tables S1–S6.

Materials and Organic Syntheses

Chemicals were purchased from Sigma Aldrich, Acros Organics, TCI, Apollo Scientific, ABCR, Alfa Aesar, Carbosynth and Fluorochem and were used as received. Solvents were purchased from Fluorochem, Fisher Chemical, and Sigma Aldrich, while deuterated solvents were from Eurisotop and Sigma Aldrich. THF, Et_2O, and CH_2Cl_2 were dried on a Braun MB SPS-800 solvent purification system. MeOH, $CHCl_3$, and acetone were purchased as reagent-grade and used without further purification. Et_3N was distilled from CaH_2 and then stored over KOH. Anhydrous dioxane and pyridine were purchased from Sigma Aldrich. Solutions of *i*-PrMgCl in THF were freshly prepared according to a procedure by Lin et al.[40] and titrated with the Paquette method[41] or directly purchased from Sigma Aldrich. Low-temperature baths were prepared using different solvent mixtures depending on the desired temperature: 0 °C with ice/H_2O. Anhydrous conditions were achieved by flaming two necked flasks with a heat gun under vacuum and purging with N_2. The inert atmosphere was maintained using N_2-cooled balloons equipped with a syringe and needle to penetrate the silicon stoppers, closing the flask's necks. Additions of liquid reagents were performed using dried plastic or glass syringes. Unless otherwise stated, all reactions were performed in dry conditions and under an inert atmosphere.

Density Functional Theory (DFT) calculations. The DFT calculations reported in this work have been performed via the mixed Gaussian and plane waves (GPW) method implemented in the CP2K package.[43] The choice of the exchange-correlation (XC) functional, which is always an important consideration when investigating molecular interactions, is especially controversial when describing chalcogenide bonds. For instance, the work of Bickelhaupt[44] recommends the usage of hybrid functionals, particularly B3LYP, as opposed to the addition of dispersion corrections to non-hybrid functionals – which might lead to overestimating the strength of chalcogen bonds. On the other hand, Goerigk argues against using B3LYP and recommends instead dispersion-corrected functionals such as the PW6B95 D3.[45] To address this conundrum, we have chosen to explore different XC functionals, namely PBE;[46] PBE-D3,[47] which feature a dispersion correction; vdW DF69,[48] which is a fully self-consistent, nonlocal XC functional and HSE06,[49] which is a hybrid functional. Goedecker-type pseudopotentials[50] with four, one, six, five, and six valence electrons for C, H, O, N, and Se, respectively, have been employed. The Kohn Sham orbitals were expanded in a triple-zeta valence plus two sets of polarisation functions (TZV2P) Gaussian-type basis set. The plane wave cutoff for the finest level of the multi-grid[43] has been set to 400 Ry to efficiently solve the Poisson equation within periodic boundary conditions using the Quickstep scheme.[43] Brillouin zone integration was restricted to the supercell Gamma point. We have found that a cubic simulation box (edge = 40 Å), introducing ~20 Å of vacuum between the periodic replica of the dimers in each direction, is sufficient to converge the total energy to 2 meV/atom. ***ALMO-EDA calculations.*** The Absolutely Localized Molecular Orbitals Energy Decomposition Analysis (ALMO-EDA) is a computational framework that can be used to investigate the different contributions to the total interaction energies we have previously discussed. This framework has been extensively reviewed elsewhere[51] and is readily available within the CP2K package. Here, it suffices to say that within the ALMO-EDA formalism, the total interaction energy E_{Tot} between two molecules can be written as:

$$E_{Tot} = E_{Frz} + E_{Pol} + E_{Cov}$$

The frozen density term (E_{Frz}) is defined as the energy change that corresponds to bringing infinitely separated molecules into the dimer geometry without any relaxation of the molecular orbitals (MOs) on the monomers. The polarization energy (E_{Pol}) is defined as the energy lowering due to the intramolecular relaxation of each molecule's ALMOs within the field of all other molecules in the system. The remaining portion of the total interaction energy is the electron delocalization or charge-transfer energy term (E_{Cov}), which is calculated as the energy difference between the state formed from the polarized ALMOs and the state constructed from the fully optimized delocalized MOs. This framework also gives access to the actual charge transfer (CT) contribution, computed as the degree of electron relaxation from the polarized state to the delocalized state. By contrast, population analysis methods include not only the "true" CT, but also the separate effect of partitioning the charge distribution of the polarized pre-CT state. Thus, the critical advantage of the ALMO approach is that it shows the electron transfer associated with the energy lowering due to dative interactions exclusively. Crucial to the correct assessment of the interaction energy is an estimate of the BSSE, which is not introduced when calculating the frozen density and the polarization energy contributions (i.e., E_{Frz} and E_{Pol}) because constrained ALMO optimization prevents electrons on one molecule from borrowing the atomic orbitals (AOs) of other molecules to compensate for the incompleteness of their own AOs. However, the BSSE does enter the charge transfer terms (i.e., E_{Cov}) since both the BSSE and charge transfer result from the same physical phenomenon of delocalization of fragment MOs. Therefore, these terms are inseparable from each other when finite Gaussian basis sets are used to describe fragments at finite spatial separation.

Synthetic procedures. To improve the yield of **3**, *t*-BuOK must be activated by flame-drying it under a vacuum for 20 minutes.

Similarly, to freshly prepare Li_2Se_2, the activation of Li^0 consists of pressing elemental lithium chunks with a test tube, then the resulting plates are washed with degassed petr. ether, dried under a flow of Ar and added to a solution of dry THF. For the synthesis of $\mathbf{1}_F$ and $\mathbf{1}_{3F}$, 2.5 equivalents of corresponding primary amine were used (rather than 1.2), which were added to the acyl chloride within 30 minutes at −40 °C.

tert-Butyl 2-chloronicotinate 3

To a two-necked 50 mL round-bottomed flask with a suspension of 2-chloronicotinic acid **2** (5 g, 31.7 mmol) in $SOCl_2$ (25 mL) under anhydrous condition, dry DMF (2 drops) was added dropwise, then the reaction heated up to reflux, stirred for 4 h and the solvents distilled off. To a two-necked 50 mL round-bottomed flask with a solution of activated *t*-BuOK (3.56 g, 31.7 mmol) in dry THF (10 mL) under anhydrous condition, a solution of the resulting acyl chloride derivative in dry THF (8 mL) was added at −15 °C over 1 h. The reaction was slowly allowed to warm up to room temperature, stirred for 16 h, then poured in cold water (30 mL) and extracted with CH_2Cl_2 (3×50 mL). The combined organic extracts were washed with brine (30 mL), dried over Na_2SO_4, filtered and the solvents evaporated *in vacuo*. The crude was purified by silica gel chromatography (CH_2Cl_2) to give pure **3** as an orange oil (4.1 g, 61 % yield).

^{1}H NMR (700 MHz, $CDCl_3$) δ: 8.45 (*d*, $J_{H,H}$ = 4.5 Hz, 1H, H_a), 8.04 (*d*, $J_{H,H}$ = 7.6 Hz, 1H, H_c), 7.28 (*d*, $J_{H,H}$ = 7.6, 4.5 Hz, 1H, H_b), 1.59 (*s*, 9H, H_d); ^{13}C NMR (175 MHz, $CDCl_3$) δ: 163.9, 151.2, 149.4, 139.7, 128.8, 122.0, 28.0; FTIR (ATR): ν (cm^{-1}): 2980, 2936, 1723, 15778, 1561, 1479, 1457, 1400, 1369, 1312, 1285, 1252, 1172, 1139, 1063, 1055, 1036, 865, 847, 819, 765, 718, 647, 543, 476, 432; HRMS (ESI): *m/z* calcd for $C_{10}H_{12}NOCl + Na^+$: 236.0449 $[M + Na]^+$; found: 236.0445.

Di-*Tert*-Butyl 2,2′-Diselanediyldinicotinate 4

To a flame-dried Schlenk tube loaded with a suspension of activated lithium (120 mg, 17.3 mmol) and 4,4'-di-*tert*-butylbiphenyl (100 mg, 0.38 mmol) in dry THF (25 mL) under anhydrous condition, a gentle vacuum was applied, and the reaction sonicated for 15 minutes (colorless turned into dark green). Freshly grounded elemental selenium (4 g, 50.7 mmol) was added while a brisk flux of N_2 was passed through the flask, then the reaction sonicated at 50 °C for 4 h. To a suspension of the resulting dilithium diselenide derivative, a solution of *t*-butyl 2–chloroquinoline-3-carboxylate **3** (720 mg, 2.74 mmol) in dry THF (8 mL) was added dropwise at −15 °C. The reaction was slowly warmed to room temperature, stirred for 72 h, quenched with MeOH (30 mL), and filtered over celite. The filtrate was concentrated under reduced pressure, MeOH (30 mL) added, and the resulting suspension centrifugated for 15 minutes (5000 rpm). The system was filtered, and the solid was washed with MeOH (2×10 mL) to give pure **4** as an orange solid (340 mg, 33 % yield). mp: 208–210 °C; ^{1}H NMR (600 MHz, $CDCl_3$) δ: 8.47 (*dd*, $J_{H,H}$ = 4.7, 1.8 Hz, 2H, H_a), 8.13 (*dd*, $J_{H,H}$ = 7.7, 1.8 Hz, 2H, H_c), 7.09 (*dd*, $J_{H,H}$ = 7.7, 4.7 Hz, 2H, H_b), 1.64 (*s*, 18H, H_d); ^{13}C NMR (150 MHz, $CDCl_3$) δ: 165.4, 161.1, 152.5, 138.2, 126.4, 119.4, 28.3; FTIR (ATR): ν (cm^{-1}): 29707, 2931, 1682, 1567, 1552, 1392, 1366, 1302, 1256, 1235, 1171, 1116, 1062, 866, 847, 821, 804, 758, 714, 648, 515, 488, 471, 418; HRMS (ESI): *m/z* calcd for $C_{20}H_{24}O_4N_2Se_2 + H^+$: 517.0139 $[M + H]^+$; found: 517.0146.

2,2′-Diselanediyldinicotinic Acid 5

To a sealed vial loaded with a solution of di-*tert*-butyl 2,2′-diselanediyldinicotinate **4** (100 mg, 0.2 mmol) in CH_2Cl_2 (8 mL), CH_3SO_3H (148 mg, 0.1 mL, 1.6 mmol) was added dropwise at room temperature. The reaction was stirred for 16 h, then quenched by MeOH (10 mL). The resulting insoluble solid was filtered and washed with MeOH (2×20 mL) and water (3×20 mL) to give pure **5** as a yellow solid (79 mg, 96 % yield). mp: 192–194 °C; ^{1}H NMR (600 MHz, DMSO-d_6) δ: 8.55 (*dd*, $J_{H,H}$ = 4.8, 1.7 Hz, 2H, H_a), 8.22 (*dd*, $J_{H,H}$ = 7.7, 1.7 Hz, 2H, H_c), 7.31 (*dd*, $J_{H,H}$ = 7.7, 4.8 Hz, 2H, H_b); ^{13}C NMR (150 MHz, DMSO–d_6) δ: 167.8, 161.6, 153.0, 138.7, 125.7, 120.4; FTIR (ATR): ν (cm^{-1}): 3140, 2855, 1663, 1569, 1548, 1445, 1421, 1383, 1300, 1238, 1225, 1150, 1120, 1064, 889, 818, 758, 705, 644, 553, 523, 476, 450, 437, 420; HRMS (ESI): *m/z* calcd for $C_{12}H_8O_4N_2Se_2 + H^+$: 404.8890 $[M + H]^+$; found: 404.8873.

2-Phenyl-[1,2]selenazolo[5,4-β]pyridin-3(2H)-One $\mathbf{1}_{Ph}$

To a two-necked 25 mL round-bottomed flask with a suspension of 2,2′-diselanediyldinicotinic acid **5** (80 mg, 0.2 mmol) in $SOCl_2$ (0.6 mL) under anhydrous condition, dry DMF (2 drops) was added dropwise, then the reaction heated up to reflux and stirred for 6 h. The reaction was cooled to room temperature, and a second portion of $SOCl_2$ (0.6 mL) and dry DMF (2 drops) were added. The solution was heated to reflux and stirred for 16 h, and then the solvents were distilled. To a solution of the resulting acyl chloride derivative in dry CH_2Cl_2 (5 mL), a solution of aniline (20 mg, 0.02 mL, 0.22 mmol) and NEt_3 (44 mg, 0.06 mL, 0.44 mmol) in dry CH_2Cl_2 (0.4 mL) was added dropwise at −15 °C. The reaction was slowly allowed to warm up to room temperature and stirred for 16 hours, then poured in cold water (30 mL) and extracted with CH_2Cl_2 (3×30 mL). The combined organic extracts were washed with brine (20 mL), dried over Na_2SO_4, filtered, and the solvents evaporated *in vacuo*. The crude was purified by silica gel chromatography ($CHCl_3$/EtOAc 3 : 1) to give pure $\mathbf{1}_{Ph}$ as a white solid (25 mg, 45 % yield). mp: 180–182 °C; ^{1}H NMR (600 MHz, $CDCl_3$) δ: 8.84 (*d*, $J_{H,H}$ = 4.5 Hz, 1H, H_a), 8.39 (*dd*, $J_{H,H}$ = 7.7, 1.7 Hz, 1H, H_c), 7.65 (*dm*, $J_{H,H}$ = 8.5 Hz, 2H, H_d), 7.49 (*d*, $J_{H,H}$ = 7.7, 4.5 Hz, 1H, H_b), 7.46 (*dd*, $J_{H,H}$ = 8.5, 7.5 Hz, 2H, H_e), 7.31 (*t*, $J_{H,H}$ = 7.5 Hz, 1H, H_f); ^{13}C NMR (150 MHz, $CDCl_3$) δ: 163.8, 161.7, 152.7, 138.8, 137.6, 129.6, 127.1, 125.7, 124.5, 122.1; ^{77}Se NMR (114 MHz, $CDCl_3$) δ: 953.8 (*s*); FTIR (ATR): ν (cm^{-1}): 3070, 2921, 2852, 1655, 1638, 1584, 1486, 1452, 1391, 1336, 1262, 1205, 1181, 1141, 1108, 1085, 943, 815, 751, 692, 672, 600, 528, 481; HRMS (ESI): *m/z* calcd for $C_{12}H_8ON_2Se + H^+$: 276.9875 $[M + H]^+$; found: 276.9873. Single crystals suitable for X-ray diffraction analysis were grown from slow solvent evaporation from a $CHCl_3$/toluene 1 : 1 solution.

2-Pentyl-[1,2]selenazolo[5,4-β]pyridin-3(2H)-One $\mathbf{1}_{Alk}$

To a two-necked 25 mL round-bottomed flask with a suspension of 2,2′-diselanediyldinicotinic acid **5** (80 mg, 0.2 mmol) in $SOCl_2$ (0.6 mL) under anhydrous condition, dry DMF (2 drops) was added dropwise, then the reaction heated up to reflux and stirred for 6 h. The reaction was cooled to room temperature, and a second portion of $SOCl_2$ (0.6 mL) and dry DMF (2 drops) were added. The solution was heated to reflux and stirred for 16 h, and the solvents were distilled. To a solution of the resulting acyl chloride derivative in dry CH_2Cl_2 (5 mL), a solution of amylamine (19 mg, 0.03 mL, 0.22 mmol) and NEt_3 (44 mg, 0.06 mL, 0.44 mmol) in dry CH_2Cl_2 (0.4 mL) was added dropwise at −15 °C. The reaction was slowly warmed to room temperature and stirred for 16 h, then poured in cold water (30 mL) and extracted with CH_2Cl_2 (3×30 mL). The combined organic extracts were washed with brine (20 mL), dried over Na_2SO_4, filtered, and the solvents evaporated *in vacuo*. The crude was purified by silica gel chromatography ($CHCl_3$/EtOAc 4 : 1) to give pure $\mathbf{1}_{Alk}$ as a white solid (38 mg, 72 % yield). mp: 138–140 °C; ^{1}H NMR (600 MHz, $CDCl_3$) δ: 8.74 (*dd*, $J_{H,H}$ = 4.9, 1.7 Hz, 1H,

H_a), 8.25 (*dd*, $J_{H,H}$ = 7.8, 1.7 Hz, 1H, H_c), 7.39 (*dd*, $J_{H,H}$ = 7.8, 4.9 Hz, 1H, H_b), 3.87 (*t*, $J_{H,H}$ = 7.2 Hz, 2H, H_d), 1.78–1.73 (*m*, 2H, H_e), 1.42–1.36 (*m*, 4H, $H_{f,g}$), 0.91 (*t*, $J_{H,H}$ = 7.2 Hz, 3H, H_h); ^{13}C NMR (150 MHz, $CDCl_3$) δ: 165.2, 161.8, 152.7, 136.5, 123.5, 121.5, 44.6, 30.2, 28.8, 22.3, 13.9; ^{77}Se NMR (114 MHz, $CDCl_3$) δ: 897.6 (*s*); FTIR (ATR): ν (cm^{-1}): 2950, 2923, 2854, 1641, 1624, 1581, 1562, 1465, 1385, 1308, 1251, 1217, 1167, 1105, 1082, 1051, 820, 755, 698, 666, 519, 490, 443; HRMS (ESI): *m/z* calcd for $C_{11}H_{14}ON_2Se + Na^+$: 293.0164 $[M + Na]^+$; found: 293.0167. Single crystals suitable for X-ray diffraction analysis were grown from slow solvent evaporation from a toluene solution.

2-(Anthracen-9-Yl)-[1,2]selenazolo[5,4-β]pyridin-3(2H)-One $\mathbf{1}_{Anthr}$

To a two-necked 25 mL round-bottomed flask with a suspension of 2,2′-diselanediyldinicotinic acid **5** (80 mg, 0.2 mmol) in $SOCl_2$ (0.6 mL) under anhydrous condition, dry DMF (2 drops) was added dropwise, then the reaction heated up to reflux and stirred for 6 h. The reaction was cooled to room temperature, and a second portion of $SOCl_2$ (0.6 mL) and dry DMF (2 drops) were added. The solution was heated to reflux and stirred for 16 h, and the solvents were distilled. To a solution of the resulting acyl chloride derivative in dry CH_2Cl_2 (5 mL), a solution of anthracen-9-amine (43 mg, 0.22 mmol) and NEt_3 (44 mg, 0.06 mL, 0.44 mmol) in dry CH_2Cl_2 (0.4 mL) was added dropwise at −15 °C. The reaction was stirred at 50 °C for 16 h, then poured in cold water (30 mL) and extracted with CH_2Cl_2 (3×30 mL). The combined organic extracts were washed with brine (20 mL), dried over Na_2SO_4, filtered, and the solvents evaporated *in vacuo*. The crude was purified by silica gel chromatography ($CHCl_3$/EtOAc 3:1) to give pure $\mathbf{1}_{Anthr}$ as a pale-yellow solid (30 mg, 41% yield). mp: >230 °C; ^{1}H NMR (600 MHz, $CDCl_3$) δ: 8.89 (*dd*, $J_{H,H}$ = 4.9, 1.7 Hz, 1H, H_a), 8.63 (*s*, 1H, H_h), 8.46 (*dd*, $J_{H,H}$ = 7.8, 1.7 Hz, 1H, H_c), 8.18 (*d*, $J_{H,H}$ = 8.6 Hz, 2H, H_d), 7.89 (*d*, $J_{H,H}$ = 8.6 Hz, 2H, H_g), 7.57 – 7.49 (*m*, 5H, $H_{b,e,f}$); ^{13}C NMR (150 MHz, $CDCl_3$) δ: 165.6, 163.2, 153.8, 137.6, 131.9, 129.7, 129.1, 128.9, 128.6, 127.4, 125.8, 123.0, 122.1, 121.8; FTIR (ATR): ν (cm^{-1}): 2979, 2363, 1639, 1579, 1560, 1463, 1409, 1391, 1366, 1233, 1083, 912, 843, 820, 782, 757, 731, 697, 671, 596, 551, 512, 476, 446, 435; HRMS (LD): *m/z* calcd for $C_{20}H_{12}ON_2Se^+$: 376.0110 $[M]^+$; found: 376.0103. Single crystals suitable for X-ray diffraction analysis were grown from slow solvent evaporation from a $CHCl_3$/toluene solution.

2-(4-Fluorophenyl)-[1,2]selenazolo[5,4-β]pyridin-3(2H)-One ($\mathbf{1}_F$)

To a two-necked 25 mL round-bottomed flask with a suspension of 2,2′-diselanediyldinicotinic acid **5** (80 mg, 0.2 mmol) in $SOCl_2$ (0.6 mL) under anhydrous condition, dry DMF (2 drops) was added dropwise, then the reaction heated up to reflux and stirred for 6 h. The reaction was cooled to room temperature, and a second portion of $SOCl_2$ (0.6 mL) and dry DMF (2 drops) were added. The solution was heated to reflux and stirred for 16 h, and the solvents were distilled. To a solution of the resulting acyl chloride derivative in dry CH_2Cl_2 (5 mL), a solution of 4-fluoroaniline (61 mg, 52 μL, 0.55 mmol) and NEt_3 (67 mg, 0.08 mL, 0.6 mmol) in dry CH_2Cl_2 (0.4 mL) was added dropwise at −40 °C. The reaction was stirred at room temperature for 8 h, then poured in cold water (30 mL) and extracted with CH_2Cl_2 (3×30 mL). The combined organic extracts were washed with brine (20 mL), dried over Na_2SO_4, filtered, and the solvents evaporated *in vacuo*. The crude was purified by silica gel chromatography ($CHCl_3$/EtOAc 5:1) to give pure $\mathbf{1}_F$ as a pale-yellow solid (13 mg, 23% yield). mp: 158–160 °C; ^{1}H NMR (400 MHz, $CDCl_3$) δ: 8.83 (*d*, $J_{H,H}$ = 4.5 Hz, 1H, H_a), 8.36 (*d*, $J_{H,H}$ = 7.7 Hz, 1H, H_c), 7.59 (*dd*, $J_{H,H}$ = 8.4, 4.8 Hz, 2H, H_d), 7.48 (*dd*, $J_{H,H}$ = 7.7, 4.5 Hz, 1H, H_b), 7.15 (*d*, $J_{H,H}$ = 8.8, 8.4 Hz, 2H, H_e); ^{19} F NMR (376 MHz, $CDCl_3$) δ: −113.80 (s, 1F); ^{13}C NMR (100 MHz, $CDCl_3$) δ: 161.6, 153.1, 137.3, 127.7, 127.6, 123.6, 122.0, 116.4, 116.2, 110.3 (*d*, $J_{C,F}$ = 250.1 Hz); FTIR (ATR): ν (cm^{-1}): 3052, 2989, 1687, 1644, 1523, 1491, 1463, 1343, 1290, 1223, 1199, 1156, 1111, 1063, 943, 889, 823, 778, 699, 616; HRMS (ESI): *m/z* calcd for $C_{12}H_7ON_2FSe + Na^+$: 316.9600 $[M + Na]^+$; found: 316.9599.

2-(4-Methoxyphenyl)-[1,2]selenazolo[5,4-β]pyridin-3(2H)-One $\mathbf{1}_{Met}$

To a two-necked 25 mL round-bottomed flask with a suspension of 2,2′-diselanediyldinicotinic acid **5** (80 mg, 0.2 mmol) in $SOCl_2$ (0.6 mL) under anhydrous condition, dry DMF (2 drops) was added dropwise, then the reaction heated up to reflux and stirred for 6 h. The reaction was cooled to room temperature, and a second portion of $SOCl_2$ (0.6 mL) and dry DMF (2 drops) were added. The solution was heated to reflux and stirred for 16 h and the solvents distilled. To a solution of the resulting acyl chloride derivative in dry CH_2Cl_2 (5 mL), a solution of 4-methoxyaniline (28 mg, 0.22 mmol) and NEt_3 (44 mg, 0.06 mL, 0.44 mmol) in dry CH_2Cl_2 (0.4 mL) were added dropwise at −15 °C. The reaction was stirred at room temperature for 16 h, then poured in cold water (30 mL) and extracted with CH_2Cl_2 (3×30 mL). The combined organic extracts were washed with brine (20 mL), dried over Na_2SO_4, filtered, and the solvents evaporated *in vacuo*. The crude was purified by silica gel chromatography ($CHCl_3$/EtOAc 4:1) to give pure $\mathbf{1}_{Met}$ as a white solid (52 mg, 85% yield). mp: 133–136 °C; ^{1}H NMR (400 MHz, $CDCl_3$) δ: 8.81 (*dd*, $J_{H,H}$ = 5.0, 1.6 Hz, 1H, H_a), 8.34 (*dd*, $J_{H,H}$ = 7.9, 1.6 Hz, 1H, H_c), 7.51 (*d*, $J_{H,H}$ = 8.8 Hz, 2H, H_d), 7.45 (*dd*, $J_{H,H}$ = 7.9, 5.0 Hz, 1H, H_b), 6.97 (*d*, $J_{H,H}$ = 8.8 Hz, 2H, H_e), 3.85 (*s*, 3H, H_f); ^{13}C NMR (100 MHz, $CDCl_3$) δ: 163.9, 161.8, 158.5, 152.7, 137.2, 131.1, 127.4, 123.9, 121.8, 114.6, 55.6; FTIR (ATR): ν (cm^{-1}): 3051, 2989, 2913, 1623, 1599, 1467, 1421, 1387, 1350, 1321, 1284, 1222, 1190, 1136, 1110, 993, 867, 801, 745, 721, 654, 572; HRMS (ESI): *m/z* calcd for $C_{13}H_{10}O_2N_2Se + H^+$: 306.9981 $[M + H]^+$; found: 306.9982. Single crystals suitable for X-ray diffraction analysis were grown from slow solvent evaporation from a $CHCl_3$/toluene solution.

2-(3,4,5-Trifluorophenyl)-[1,2]selenazolo[5,4-β]pyridin-3(2H)-One $\mathbf{1}_{3F}$

To a two-necked 25 mL round-bottomed flask with a suspension of 2,2′-diselanediyldinicotinic acid **5** (80 mg, 0.2 mmol) in $SOCl_2$ (0.6 mL) under anhydrous condition, dry DMF (2 drops) was added dropwise, then the reaction heated up to reflux and stirred for 6 h. The reaction was cooled down to room temperature, and a second portion of $SOCl_2$ (0.6 mL) and dry DMF (2 drops) was added. The solution was heated up to reflux and stirred for 16 h and the solvents were distilled. To a solution of the resulting acyl chloride derivative in dry CH_2Cl_2 (5 mL), a solution of 3,4,5-trifluoroaniline (81 mg, 0.55 mmol) and NEt_3 (67 mg, 0.08 mL, 0.6 mmol) in dry CH_2Cl_2 (0.4 mL) was added dropwise at −40 °C. The reaction was stirred at room temperature for 10 h, then poured in cold water (30 mL) and extracted with CH_2Cl_2 (3×30 mL). The combined organic extracts were washed with brine (20 mL), dried over Na_2SO_4, filtered and the solvents evaporated *in vacuo*. The crude was purified by silica gel chromatography ($CHCl_3$/EtOAc 3:1) to give pure $\mathbf{1}_{3F}$ as a white solid (14 mg, 21% yield). mp: 176–178 °C; ^{1}H NMR (400 MHz, $CDCl_3$) δ: 8.83–8.82 (*m*, 1H, H_a), 8.34–8.32 (*m*, 1H, H_c), 7.52–7.49 (*m*, 1H, H_b), 7.39–7.36 (*m*, 2H, H_d); ^{19}F NMR (659 MHz, DMSO-d_6) δ: −134.28 (*d*, $J_{F,F}$ = 22.08 Hz, 2F), −164.45 (*t*, $J_{F,F}$ = 22.08 Hz, 1F); ^{13}C analysis is missing due to the poor solubility of the targeted molecule in several solvents screened; FTIR (ATR): ν (cm^{-1}): 3098, 2923, 2887, 1710, 1643, 1552, 1491, 1413, 1392, 1337, 1289, 1238, 1154, 1113, 1062, 983, 907, 826, 796, 701, 592, 478, 452;

HRMS (ESI): *m/z* calcd for $C_{12}H_5ON_2F_3Se+H^+$: 330.9592 $[M+H]^+$; found: 330.9594.

2-(3,4,5-Trimethoxyphenyl)-[1,2]selenazolo[5,4-β] pyridin-3(2H)-One 1_{3Met}

To a two-necked 25 mL round-bottomed flask with a suspension of 2,2′-diselanediyldinicotinic acid **5** (80 mg, 0.2 mmol) in $SOCl_2$ (0.6 mL) under anhydrous condition, dry DMF (2 drops) was added dropwise, then the reaction heated up to reflux and stirred for 6 h. The reaction was cooled to room temperature, and a second portion of $SOCl_2$ (0.6 mL) and dry DMF (2 drops) were added. The solution was heated to reflux and stirred for 16 h and the solvents distilled. To a solution of the resulting acyl chloride derivative in dry CH_2Cl_2 (5 mL), a solution of 3,4,5-trimethoxyaniline (40 mg, 0.22 mmol) and NEt_3 (44 mg, 0.06 mL, 0.44 mmol) in dry CH_2Cl_2 (0.4 mL) was added dropwise at −15 °C. The reaction was stirred at room temperature for 16 h, then poured in cold water (30 mL) and extracted with CH_2Cl_2 (3×30 mL). The combined organic extracts were washed with brine (20 mL), dried over Na_2SO_4, filtered, and the solvents evaporated *in vacuo*. The crude was purified by silica gel chromatography ($CHCl_3$/EtOAc 4:1) to give pure $\mathbf{1}_{3Met}$ as a white solid (64 mg, 88% yield). mp: 141–143 °C; ^{1}H NMR (400 MHz, $CDCl_3$) δ: 8.83 (*d*, $J_{H,H}$ = 4.7 Hz, 1H, H_a), 8.36 (*d*, $J_{H,H}$ = 7.8 Hz, 1H, H_c), 7.49 (*dd*, $J_{H,H}$ = 7.8, 4.7 Hz, 1H, H_b), 6.85 (*s*, 2H, H_d), 3.89 (*s*, 6H, H_e), 3.87 (*s*, 3H, H_f); ^{13}C NMR (100 MHz, $CDCl_3$) δ: 163.9, 161.8, 153.6, 152.9, 137.3, 137.2, 134.0, 123.9, 122.0, 103.7, 60.9, 56.3; FTIR (ATR): ν (cm^{-1}): 3030, 2984, 2916, 1621, 1589, 1515, 1438, 1367, 1329, 1251, 1222, 1167, 1098, 1003, 965, 891, 744, 639, 588; HRMS (ESI): *m/z* calcd for $C_{15}H_{14}O_4N_2Se+H^+$: 367.0192 $[M+H]^+$; found: 367.0197. Single crystals suitable for X-ray diffraction analyses were grown from the slow evaporation of solvent from a $CHCl_3$/toluene solution.

Acknowledgements

D.B. gratefully acknowledges the EU through the funding scheme projects H2020-NMBP-2017 DECOCHROM (N°760973), MSCA-ITN-ETN STiBNite ((N°956923(), and the University of Vienna for the financial support. G.C.S. gratefully acknowledges using high-performance computing (HPC) facilities, including the Sulis Tier 2 HPC platform hosted by the Scientific Computing Research Technology Platform at the University of Warwick. Sulis is funded by EPSRC Grant EP/T022108/1 and the HPC Midlands+ consortium.

Conflict of Interests

The authors declare no conflict of interest.

Data Availability Statement

The data that support the findings of this study are available from the corresponding author upon reasonable request.

Keywords: Chalcogen bonding · X-ray diffraction · Self-assembly · Dimerization

[1] N. W. Alcock, *Adv. Inorg. Chem. Radiochem.*, Elsevier **1972**, *15*, 1–58.
[2] C. B. Aakeroy, D. L. Bryce, G. R. Desiraju, A. Frontera, A. C. Legon, F. Nicotra, K. Rissanen, S. Scheiner, G. Terraneo, P. Metrangolo, *Pure Appl. Chem.* **2019**, *91*, 1889–1892.
[3] a) A. F. Cozzolino, P. J. Elder, I. Vargas-Baca, *Coord. Chem. Rev.* **2011**, *255*, 1426–1438; b) P. Politzer, J. S. Murray, T. Clark, *Phys. Chem. Chem. Phys.* **2013**, *15*, 11178–11189; c) V. Oliveira, D. Cremer, E. Kraka, *J. Phys. Chem. A* **2017**, *121*, 6845–6862; d) D. J. Pascoe, K. B. Ling, S. L. Cockroft, *J. Am. Chem. Soc.* **2017**, *139*, 15160–15167; e) S. Bhandary, A. Sirohiwal, R. Kadu, S. Kumar, D. Chopra, *Cryst. Growth Des.* **2018**, *18*, 3734–3739; f) P. C. Ho, J. Z. Wang, F. Meloni, I. Vargas-Baca, *Coord. Chem. Rev.* **2020**, *422*, 213464; g) Y. Xu, V. Kumar, M. J. Bradshaw, D. L. Bryce, *Cryst. Growth Des.* **2020**, *20*, 7910–7920; h) D. Romito, P. C. Ho, I. Vargas-Baca, D. Bonifazi, in *Chalcogen Chemistry: Fundamentals and Applications, The Royal Society of Chemistry* **2023**, 494–528; i) Q. Zhang, K. Luo, W. Zhou, A. Li, Q. He, *J. Am. Chem. Soc.* **2024**, *146*, 3635–3639; j) J. T. Wilmore, P. D. Beer, *Adv. Mater.* **2024**, *36*, 2309098.
[4] a) N. Biot, D. Bonifazi, *Chem. Eur. J.* **2018**, *24*, 5439–5443; b) M. Fourmigué, A. Dhaka, *Coord. Chem. Rev.* **2020**, *403*, 213084; c) E. Parisi, A. Carella, F. Borbone, F. Chiarella, F. S. Gentile, R. Centore, *CrystEngComm* **2022**, *24*, 2884–2890; d) D. Romito, D. Bonifazi, *Helv. Chim. Acta* **2023**, *106*, e202200159; e) J. Alfuth, O. Jeannin, M. Fourmigué, *CrystEngComm* **2023**, *25*, 5316–5323; f) A. A. Artemjev, A. S. Kubasov, V. P. Zaytsev, A. V. Borisov, A. S. Kritchenkov, V. G. Nenajdenko, R. M. Gomila, A. Frontera, A. G. Tskhovrebov, *Cryst. Growth Des.* **2023**, *23*, 2018–2023.
[5] a) J. Fanfrlík, A. Přáda, Z. Padělková, A. Pecina, J. Macháček, M. Lepšík, J. Holub, A. Růžička, D. Hnyk, P. Hobza, *Angew. Chem. Int. Ed.* **2014**, *53*, 10139–10142; b) A. Kremer, A. Fermi, N. Biot, J. Wouters, D. Bonifazi, *Chem. Eur. J.* **2016**, *22*, 5665–5675; c) H.-T. Huynh, O. Jeannin, M. Fourmigué, *Chem. Commun.* **2017**, *53*, 8467–8469; d) E. A. Chulanova, E. A. Radiush, I. K. Shundrina, I. Y. Bagryanskaya, N. A. Semenov, J. Beckmann, N. P. Gritsan, A. V. Zibarev, *Cryst. Growth Des.* **2020**, *20*, 5868–5879; e) D. Romito, N. Biot, F. Babudri, D. Bonifazi, *New J. Chem.* **2020**, *44*, 6732–6738; f) A. Dhaka, O. Jeannin, E. Aubert, E. Espinosa, M. Fourmigue, *Chem. Commun.* **2021**, *57*, 4560–4563; g) A. Dhaka, I. R. Jeon, O. Jeannin, E. Aubert, E. Espinosa, M. Fourmigué, *Angew. Chem. Int. Ed.* **2022**, *61*, e202116650; h) A. Dhaka, I.-R. Jeon, M. Fourmigué, *Acc. Chem. Res.* **2024**, *57*, 8467–8469.
[6] a) B. J. Eckstein, L. C. Brown, B. C. Noll, M. P. Moghadasnia, G. J. Balaich, C. M. McGuirk, *J. Am. Chem. Soc.* **2021**, *143*, 20207–20215; b) D. Romito, E. Fresta, L. M. Cavinato, H. Kählig, H. Amenitsch, L. Caputo, Y. Chen, P. Samorì, J. C. Charlier, R. D. Costa, D. Bonifazi, *Angew. Chem. Int. Ed.* **2022**, *61*, e202202137; c) T. Shimajiri, H. P. J. de Rouville, V. Heitz, T. Akutagawa, T. Fukushima, Y. Ishigaki, T. Suzuki, *Synlett* **2023**, *34*, 1978–1990.
[7] a) J. Y. Lim, I. Marques, A. L. Thompson, K. E. Christensen, V. Félix, P. D. Beer, *J. Am. Chem. Soc.* **2017**, *139*, 3122–3133; b) L. Vogel, P. Wonner, S. M. Huber, *Angew. Chem. Int. Ed.* **2019**, *58*, 1880–1891; c) T. Bunchuay, A. Docker, U. Eiamprasert, P. Surawatanawong, A. Brown, P. D. Beer, *Angew. Chem. Int. Ed.* **2020**, *59*, 12007–12012; d) V. A. Aliyeva, A. V. Gurbanov, A. G. Mahmoud, R. M. Gomila, A. Frontera, K. T. Mahmudov, A. J. Pombeiro, *Faraday Discuss.* **2023**, *244*, 77–95; e) S. Jia, H. Ye, P. He, X. Lin, L. You, *Nat. Commun.* **2023**, *14*, 7139; f) A. A. Sysoeva, A. S. Novikov, V. V. Suslonov, D. S. Bolotin, M. V. Il'in, *Inorg. Chim. Acta* **2024**, *561*, 121867; g) P. Pale, V. Mamane, *ChemPhysChem* **2023**, *24*, e202200481.
[8] a) J. N. Arokianathar, A. B. Frost, A. M. Slawin, D. Stead, A. D. Smith, *ACS Catal.* **2018**, *8*, 1153–1160; b) R. Weiss, E. Aubert, P. Peluso, S. Cossu, P. Pale, V. Mamane, *Molecules* **2019**, *24*, 4484; c) V. Mamane, P. Peluso, E. Aubert, R. Weiss, E. Wenger, S. Cossu, P. Pale, *Organometallics* **2020**, *39*, 3936–3950; d) L. Groslambert, A. Padilla-Hernandez, R. Weiss, P. Pale, V. Mamane, *Chem. Eur. J.* **2023**, *29*, e202203372.
[9] E. R. Robinson, C. Fallan, C. Simal, A. M. Slawin, A. D. Smith, *Chem. Sci.* **2013**, *4*, 2193–2200.
[10] a) S. Benz, J. López, J. J. Ss, J. Mareda, N. Sakai, S. Matile, *Angew. Chem. Int. Ed.* **2017**, *56*, 812–815; b) P. Wonner, A. Dreger, L. Vogel, E. Engelage, S. M. Huber, *Angew. Chem. Int. Ed.* **2019**, *58*, 16923–16927; c) P. Wonner, T. Steinke, S. M. Huber, *Synlett* **2019**, *30*, 1673–1678; d) C. M. Young, A. Elmi, D. J. Pascoe, R. K. Morris, C. McLaughlin, A. M. Woods, A. B. Frost, A. De La Houpliere, K. B. Ling, T. K. Smith, A. M. Slawin, P. H. Willoughby, S. L. Cockroft, A. D. Smith, *Angew. Chem. Int. Ed.* **2020**, *59*, 3705–3710; e) X. He, X. Wang, Y.-L. S. Tse, Z. Ke, Y.-Y. Yeung, *ACS Catal.* **2021**, *11*, 12632–12642; f) Z. Zhao, Y. Wang, *Acc. Chem. Res.* **2023**, *56*, 608–621; g) P. Pale, V. Mamane, *Chem. Eur. J.* **2023**, *29*, e202302755; h) L. Cao, H.

Chen, H. Fu, J. Xian, H. Cao, X. Pan, J. Wu, *Chem. Commun.* **2024**, *60*, 1321–1324.
[11] a) G. E. Garrett, G. L. Gibson, R. N. Straus, D. S. Seferos, M. S. Taylor, *J. Am. Chem. Soc.* **2015**, *137*, 4126–4133; b) M. Macchione, M. Tsemperouli, A. Goujon, A. R. Mallia, N. Sakai, K. Sugihara, S. Matile, *Helv. Chim. Acta* **2018**, *101*, e1800014.
[12] A. F. Cozzolino, I. Vargas-Baca, S. Mansour, A. H. Mahmoudkhani, *J. Am. Chem. Soc.* **2005**, *127*, 3184–3190.
[13] A. F. Cozzolino, G. Dimopoulos-Italiano, L. M. Lee, I. Vargas-Baca, *Eur. J. Inorg. Chem.* **2013**, *2013*, 2751–2756.
[14] M. Risto, R. W. Reed, C. M. Robertson, R. Oilunkaniemi, R. S. Laitinen, R. T. Oakley, *Chem. Commun.* **2008**, *28*, 3278–3280.
[15] L. J. Riwar, N. Trapp, K. Root, R. Zenobi, F. Diederich, *Angew. Chem. Int. Ed.* **2018**, *57*, 17259–17264.
[16] a) P. C. Ho, P. Szydlowski, J. Sinclair, P. J. Elder, J. Kübel, C. Gendy, L. M. Lee, H. Jenkins, J. F. Britten, D. R. Morim, *Nat. Commun.* **2016**, *7*, 11299; b) P. C. Ho, J. Rafique, J. Lee, L. M. Lee, H. A. Jenkins, J. F. Britten, A. L. Braga, I. Vargas-Baca, *Dalton Trans.* **2017**, *46*, 6570–6579; c) J. Wang, P. C. Ho, M. G. Craig, A. Cevallos, J. F. Britten, I. Vargasn-Baca, *Chem. Eur. J.* **2024**, *30*, e202302538.
[17] W. Wang, H. Zhu, S. Liu, Z. Zhao, L. Zhang, J. Hao, Y. Wang, *J. Am. Chem. Soc.* **2019**, *141*, 9175–9179.
[18] a) N. Biot, D. Bonifazi, *Chem. Eur. J.* **2020**, *26*, 2904–2913; b) N. Biot, D. Romito, D. Bonifazi, *Cryst. Growth Des.* **2020**, *21*, 536–543.
[19] L. Dupont, O. Dideberg, P. Jacquemin, *Acta Crystallogr. Sect. C: Cryst. Struct. Commun.* **1990**, *46*, 484–486.
[20] K. Kloc, I. Maliszewska, J. Młochowski, *Synth. Commun.* **2003**, *33*, 3805–3815.
[21] M. Giurg, J. Młochowski, *Synth. Commun.* **1999**, *29*, 2281–2291.
[22] Deposition numbers 2333906 (for $\mathbf{1}_{Ph}$), 2333906 (for $\mathbf{1}_{Ph}$), 2333763 (for $\mathbf{1}_{Alk}$), 2333913 (for $\mathbf{1}_{Anthr}$), 2333910 (for $\mathbf{1}_{Met}$), 2223676 (for $\mathbf{1}_{3F}$) and 2333762 (for $\mathbf{1}_{3Met}$) contain the supplementary crystallographic data for this paper. These data are provided free of charge by the joint Cambridge Crystallographic Data Centre and Fachinformationszentrum Karlsruhe Access Structures service.
[23] a) J. Wang, P. C. Ho, M. G. J. Craig, A. Cevallos, J. F. Britten, I. Vargas-Baca, *Chem. Eur. J.* **2023**, *30*, e202302538; b) S. Jain, S. S. Satpute, R. K. Jha, M. S. Patel, S. Kumar, *Chem. Eur. J.* **2024**, *30*, e202303289.
[24] P. Kuzmič, *Anal. Biochem.* **1996**, *237*, 260–273.
[25] a) W. Saenger, *Principles of Nucleic Acid Structure*, Springer, Heidelberg **1984**; b) J. Sartorius, H. J. Schneider, *Chem. Eur. J.* **1996**, *2*, 1446–1452.
[26] R. Z. Khaliullin, T. D. Kühne, *Phys. Chem. Chem. Phys.* **2013**, *15*, 15746–15766.
[27] R. Z. Khaliullin, A. T. Bell, M. Head-Gordon, *Chem. Eur. J.* **2009**, *15*, 851–855.
[28] R. K. Harris, E. D. Becker, S. M. Cabral De Menezes, P. Granger, R. E. Hoffman, K. W. Zilm, *Pure Appl. Chem.* **2008**, *80*, 59–84.
[29] Bruker SAINT v8.38B Copyright © 2005–2019 Bruker AXS.
[30] G. M. Sheldrick, University of Göttingen, Germany **1996**.
[31] O. V. Dolomanov, L. J. Bourhis, R. J. Gildea, J. A. Howard, H. Puschmann, *J. Appl. Crystallogr.* **2009**, *42*, 339–341.
[32] C. B. Hübschle, G. M. Sheldrick, B. Dittrich, *J. Appl. Crystallogr.* **2011**, *44*, 1281–1284.
[33] G. M. Sheldrick, SHELXS v 2016/4 University of Göttingen, Germany **2015**.
[34] A. L. Spek, *Acta Crystallogr.* **2009**, *D65*, 148–155.
[35] A. Lausi, M. Polentarutti, S. Onesti, J. Plaisier, E. Busetto, G. Bais, L. Barba, A. Cassetta, G. Campi, D. Lamba, *Eur. Phys. J. Plus* **2015**, *130*, 1–8.
[36] W. Kabsch, *Acta Crystallogr. Sect. D* **2010**, *66*, 125–132.
[37] O. V. Dolomanov, L. J. Bourhis, R. J. Gildea, J. A. Howard, H. Puschmann, *J. Appl. Crystallogr.* **2009**, *42*, 339–341.
[38] G. M. Sheldrick, *Acta Crystallogr. Sect. A Found. Adv.* **2015**, *71*, 3–8.
[39] G. M. Sheldrick, *Acta Crystallogr. Sect. C Struct. Chem.* **2015**, *71*, 3–8.
[40] W. Lin, L. Chen, P. Knochel, *Tetrahedron* **2007**, *63*, 2787–2797.
[41] H.-S. Lin, L. A. Paquette, *Synth. Commun.* **1994**, *24*, 2503–2506.
[42] P. Kuzmič, *Anal. Biochem.* **1996**, *237*, 260–273.
[43] J. VandeVondele, M. Krack, F. Mohamed, M. Parrinello, T. Chassaing, J. Hutter, *Comput. Phys. Commun.* **2005**, *167*, 103–128.
[44] L. de Azevedo Santos, T. C. Ramalho, T. A. Hamlin, F. M. Bickelhaupt, *J. Comput. Chem.* **2021**, *42*, 688–698.
[45] N. Mehta, T. Fellowes, J. M. White, L. Goerigk, *J. Chem. Theory Comput.* **2021**, *17*, 2783–2806.
[46] J. P. Perdew, K. Burke, M. Ernzerhof, *Phys. Rev. Lett.* **1996**, *77*, 3865.
[47] S. Grimme, J. Antony, S. Ehrlich, H. Krieg, *J. Chem. Phys.* **2010**, *132*, 154104.
[48] M. Dion, H. Rydberg, E. Schröder, D. C. Langreth, B. I. Lundqvist, *Phys. Rev. Lett.* **2004**, *92*, 246401.
[49] A. V. Krukau, O. A. Vydrov, A. F. Izmaylov, G. E. Scuseria, *J. Chem. Phys.* **2006**, *125*, 224106.
[50] S. Goedecker, M. Teter, J. Hutter, *Phys. Rev. B.* **1996**, *54*, 1703.
[51] R. Z. Khaliullin, E. A. Cobar, R. C. Lochan, A. T. Bell, M. Head-Gordon, *J. Phys. Chem. A* **2007**, *111*, 8753–8765.

Manuscript received: April 4, 2024
Accepted manuscript online: July 26, 2024
Version of record online: October 16, 2024